



Influence of thermal treatment regime on the density and reactivity of activated carbons from almond shells

A. Marcilla*, S. García-García, M. Asensio, J.A. Conesa

Department of Chemical Engineering, University of Alicante, P.O. Box 99, 03080 Alicante, Spain

Received 25 January 1999; accepted 18 May 1999

Abstract

A study of the influence of two successive thermal treatments, at low ($3\text{--}4^\circ\text{C min}^{-1}$) and high (ca. $3000^\circ\text{C min}^{-1}$) heating rate, on the properties and reactivity of chars obtained from almond shells was carried out. The combined thermal treatment consisted of a first stage at intermediate temperatures from 275 to 400°C at the low heating rate, followed by a second stage at the high rate, up to 850°C . All the samples obtained under these conditions (except the sample obtained at an intermediate temperature of 400°C) yielded a density much lower than that corresponding to a single thermal treatment up to 850°C at both heating rates. The sample obtained at 400°C behaved in a very interesting manner since its density was the highest obtained. A correlation has been obtained between the high reactivity of the samples obtained by a single treatment at high heating rate, and the Ca content and dispersion. The adsorption properties of the activated carbons obtained at approximately 50% burn-off were very similar regardless of the reactivity and the porous structure of the precursor chars. © 2000 Elsevier Science Ltd. All rights reserved.

Keywords: A. Char; B. Heat treatment; D. Mechanical properties; Reactivity

1. Introduction

Activated carbons are usually prepared by carbonisation of carbonaceous materials followed by activation with steam or carbon dioxide. During the carbonisation process, graphitic crystallites are formed and are irregularly arranged, which affects the porous structure of the final activated carbons.

Some authors [1] have verified the influence of the carbonisation rate in the gasification reactions. For example, it has been observed that, when the heating rate in the carbonisation step increases, the reactivity with respect to the activating agent increases, and the particle resistance decreases. However, there are not many studies concerning the effect of heating rate on the quality of the activated carbons. This work completes previous studies [2] providing more detailed knowledge of the possible effect of the carbonisation conditions on the reactivity, pore structure, density, and mechanical strength of the activated carbons obtained.

The paper focuses specifically on the following aspects:

- The effect of the combined treatment of carbonisation (a low heating rate step followed by a high heating rate step) on the physical and textural properties of the carbons obtained.
- The influence of the heating rate in the carbonisation process on the activation rate and textural properties of the activated carbons obtained
- The possible influence of the inorganic compounds present in the sample on the activation properties.

2. Experimental

In order to achieve these objectives, a set of conditions was used to prepare the chars. The carbonisation temperatures, the heating rate of the carbonization step and the time for the activation process were varied.

The reactor used, which is shown in Fig. 1, is made of stainless-steel AISI 310, and is 70 cm high with a 5.2 cm internal diameter. The reactor includes, before the distributor, a system for pre-heating the inert or reactive gas

*Corresponding author.

E-mail address: antonio.marcilla@ua.es (A. Marcilla)

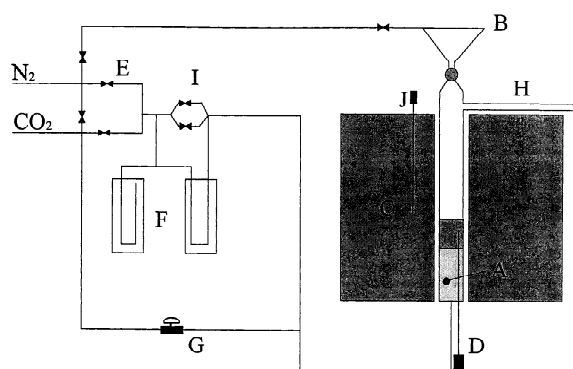


Fig. 1. Diagram of the experimental reactor. (A) gas preheater, (B) feed hopper, (C) furnace, (D, J) thermocouples, (E) gas flow valves, (F) manometers, (G) electrically operated valve, (H) gas outlet, (I) orifices for flow measurement.

in a bed of ceramic spheres. An electric furnace is controlled by two thermocouples: one of them is placed near the sample and the other inside the furnace. The system, furnace+reactor, can be rotated 180° by means of an axis allowing the discharge of the reactor. The system has the possibility of running both high (flash) and low heating rate experiments. More details about the reactor can be found elsewhere [2].

The feed material was almond shell (0.45% ash) washed with distilled water, dried, crushed and sieved. The fraction of 1.5–2.0 mm particle size was selected for the experiments.

The carbonisation runs under combined thermal treatment were performed in two stages. Sample amounts around 100 g were placed in the reactor and heated up to different final temperatures (ranging from 275 to 400°C) at a low heating rate ($3\text{--}4^\circ\text{C min}^{-1}$). The final temperature was maintained for 60 min and the sample was then cooled to room temperature. The second step consisted of pouring the char previously obtained (once the air was evacuated) into the reactor that is already at the final temperature of 850°C . This step is followed by 60 min at 850°C . The nitrogen flow in the carbonisation step was 3.1 mmol s^{-1} .

After the two stages, the samples were weighed to obtain the corresponding yield. In all the runs, the gas pressures were atmospheric.

A heating rate of ca. $3000^\circ\text{C min}^{-1}$ has been estimated for this step from the rate of evolution of volatiles and the temperature profiles. In previous studies with a stainless-steel fluidized bed reactor [3], a heating rate of $18\,000^\circ\text{C min}^{-1}$ was estimated. In this case, the heating rate was somewhat lower probably because in this case the bed was not fluidized.

Table 1 presents the carbonisation and activation conditions used in the different experiments, as well as the nomenclature, where 'L' stands for the low heating rate, 'F' for the high heating rate (flash), and 'A' for the activated carbons prepared. The number following these letters represents the final temperature of the respective treatment (i.e. L and F) and the activation time (i.e. after A). For instance, the char named as L275F850 was prepared at low heating rate to 275°C , and then at high heating rate to 850°C . L275F850A3.2 means that the char L275F850 was activated for 3.2 h.

In addition, a study was made of two chars prepared in a single stage, both at a low heating rate and at a high heating rate up to 850°C final temperature, followed by 60 min at the final temperature.

The activation of the chars was performed in the same reactor, using CO_2 as the activating agent, at 0.31 mmol s^{-1} flow rate. The activation temperatures were 780°C in the case of carbonisation in two stages, and 800 and 755°C in the case of carbons L850A4 and F850A5, respectively. The time for activation was selected in order to obtain a burn-off level close to 50%.

A Quantachrome Autosorb-6 was used to obtain 77 K nitrogen and 273 K carbon dioxide adsorption isotherms.

Micrographs of the chars were obtained with a Phillips-PSEM 55 apparatus. The particle size was obtained by measuring the average equivalent diameter (diameter of a circular particle of the same cross-sectional area as the particle considered), using a photographic system, counting and measuring a representative amount of particles.

Characterisation of the mechanical resistance was done by the measurement of the ultimate pressure (i.e. force/

Table 1
Carbonisation and activation conditions for the runs performed

Sample	Carbonisation (T ($^\circ\text{C}$)/heating rate)		Activation [T ($^\circ\text{C}$)/ t (h)]
	Stage 1	Stage 2	
L275F850A3.2	275//low	850//flash	780//3.2
L285F850A3.7	285//low	850//flash	780//3.7
L300F850A4.2	300//low	850//flash	780//4.2
L400F850A4	400//low	850//flash	780//4.0
L850A4	850//low	—	800//4.0
L850A3	850//low	—	800//3.0
F850A5	—	850//flash	755//5.0
F850A3	—	850//flash	755//3.0

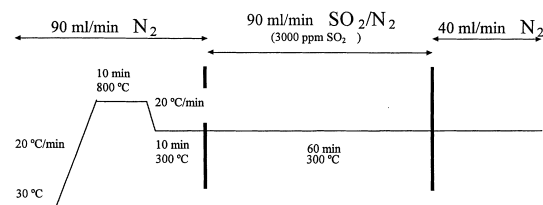


Fig. 2. Conditions of the analysis of retention of SO_2 .

projected area of the particles) before rupture of any of the three particles under study, and repeating the experiment for statistical reliability.

Studies of the retention of SO_2 were performed in a thermobalance (TG-ATD Stanton Redcroft series 780) at 573 K, using a mixture of 0.3% v/v of SO_2 in N_2 as the reaction gas, at atmospheric pressure. The conditions of the

analysis are shown in Fig. 2. These conditions are those recommended for this type of analysis [4].

3. Results and discussion

3.1. Char yield and reactivity of the activated particles.

Table 2 shows the yields of the first and second stages of carbonisation and the burn-off of the activated samples obtained from each char. These parameters were calculated using the following equations:

Yield of the first stage: $Y1$ (%)

$$= \frac{\text{(weight of the char from the first stage)}}{\text{(weight of the almond shell)}} \times 100$$

Table 2

Yields of the first and second stage of carbonisation and the burn-off of the activated samples

Sample	$Y1$ (%)	$Y2$ (%)	Y_G (%)	BO (%)	Diameter ^a (mm)	Density ^a (g cm^{-3})
L275F850A3.2	59.64	38.55	22.99	44.91	2.42	—
L285F850A3.7	53.59	45.09	24.16	48.78	2.26	—
L300F850A4.2	40.65	59.41	24.15	53.89	2.12	0.465
L325F850A4	40.44	64.38	25.87	47.31	1.84	0.695
L400F850A4	34.63	76.07	26.34	49.99	1.05	1.242
L850A4	—	—	23.13	59.19		
F850A5	—	—	15.84	56.60		
L850A3	—	—	23.13	38.01		
F850A3	—	—	15.84	38.80		

^a Diameter or density of the chars obtained in the second stage of carbonisation.

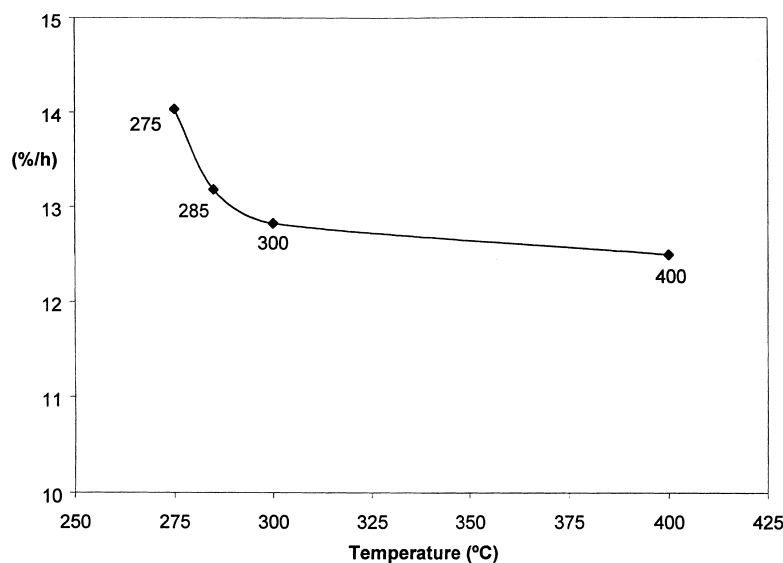


Fig. 3. Reactivities during the activation process as a function of the temperature of the first stage of carbonisation.

Yield of the second stage: Y_2 (%)

$$= (\text{weight of the char from the second stage}) / (\text{weight of the char from the first stage}) \times 100$$

Global yield of the process: Y_G (%) = $Y_1 \times Y_2 / 100$

Burn-off: BO (%) = $[1 - (\text{weight of the activated carbon} / \text{weight of char})] \times 100$

Reactivity: $R = BO / (\text{time of activation})$

The yield of the process of carbonisation is mainly determined by the dehydration reactions of the lignocellulosic material [5], which are a function of both the precursor and the experimental conditions used. As observed in Table 2, the sample F850 has the lowest global yield of all the samples studied, corresponding to the more severe thermal treatment. These results are in good agreement with those obtained by other authors when comparing the yields from flash and low heating rates carbonisation processes [6].

Fig. 3 shows the reactivity as a function of the temperature of the first stage of carbonisation, where a clear trend can be observed. The reactivity increases as the intensity of the flash treatment increases (i.e. the temperature of the first stage decreases). This result is the expected one, since according to other authors [5,6], the chars obtained under flash are much more reactive than those obtained by a slow heating rate treatment. The reactivity of the samples obtained in the present work under combined treatment must lie between those of the pure flash and pure slow heating rate treatments. From the data in Tables 1 and 2, the reactivity of the chars obtained in the pure flash and in pure slow treatment can be compared. The runs performed at the same activation time (L850A3 and F850A3) show clearly that the reactivity of the pure flash char is higher than that of the pure slow treatment char, since the burn-offs are similar, but the temperature of activation of the pure flash is much lower (i.e. 755 vs. 800°C).

3.2. Adsorption data.

The N_2 (at 77 K) and CO_2 (at 273 K) adsorption isotherms of the chars and the activated carbons with a burn-off close to 50% were obtained in a volumetric system (Quantachrome, Autosorb-6). Figs. 4 and 5 show the adsorption isotherms. Table 3 shows the specific surface areas (resulting from the application of the Dubinin-Radushkevich (D.R.) equation [7]) of the activated and carbonised samples obtained. Comparing the N_2 and CO_2 isotherms for these chars, it can be concluded that the carbonised sample obtained under the single flash treatment (F850) exhibits diffusion problems, yielding

values of the surface area using nitrogen much lower than the sample obtained using carbon dioxide (see Table 3). Nevertheless, this sample is very reactive (i.e. much more reactive than the char obtained under the pure low heating rate treatment) proving that there is no straightforward relationship between the porous structure of the chars and their reactivities. Moreover, the surface area of the corresponding activated carbon is similar to the rest of the samples (and even higher) despite the low surface area of the char obtained from nitrogen adsorption.

The differences between the CO_2 adsorption isotherms are smaller than the differences between the N_2 isotherms. This fact would support more similar reactivities between the samples when activating with CO_2 . From all this, it can be concluded that the reactivity of the carbonised samples must be the result of a complex combination of different factors.

The areas of the different activated carbons, calculated for the same burn-off, are also very similar, as well as the shape of the isotherms.

3.3. Average diameter and resistance.

Fig. 6 shows the average diameter of the carbonised particles as a function of the temperature of the first stage. In order to test the correlation between the diameter measured and the density, the density of three selected chars was measured using a mercury porosimeter. Table 2 shows the results (diameter, density), and a clear linear correlation between these variables exists with the following equation [diameter (mm) = $2.0011 - 0.7188 \times \text{density (g cm}^{-3})$], correlation coefficient = 0.9986]. As can be seen in Fig. 6, the chars obtained in two stages, in which the temperature of the first stage was between 275°C and 300°C, show a marked decrease in density (which is much lower than that of the L850 and F850). On the other hand, the sample L400F850 was denser than the single treatment chars. The diameter of the raw material is also shown for comparison purposes.

Fig. 7 shows the mechanical resistance of the activated samples. Following this figure and Fig. 6, it can be observed that the decrease in density (or the associated increase in particle diameter) is closely related to the decrease in the mechanical resistance. On the other hand, the increase in density of the particles (sample L400) produces a noteworthy increase of the mechanical resistance. This result can be of great practical importance since it means that very interesting products can be obtained by adequate combined thermal treatment, producing particles that are denser, more resistant, more reactive and with similar adsorption capacity to those obtained by the slow heating treatment. This offers an interesting alternative to the low mechanical strength of the flash activated carbons.

With respect to the samples obtained in one stage, the mechanical resistance of the sample L850A4 is greater

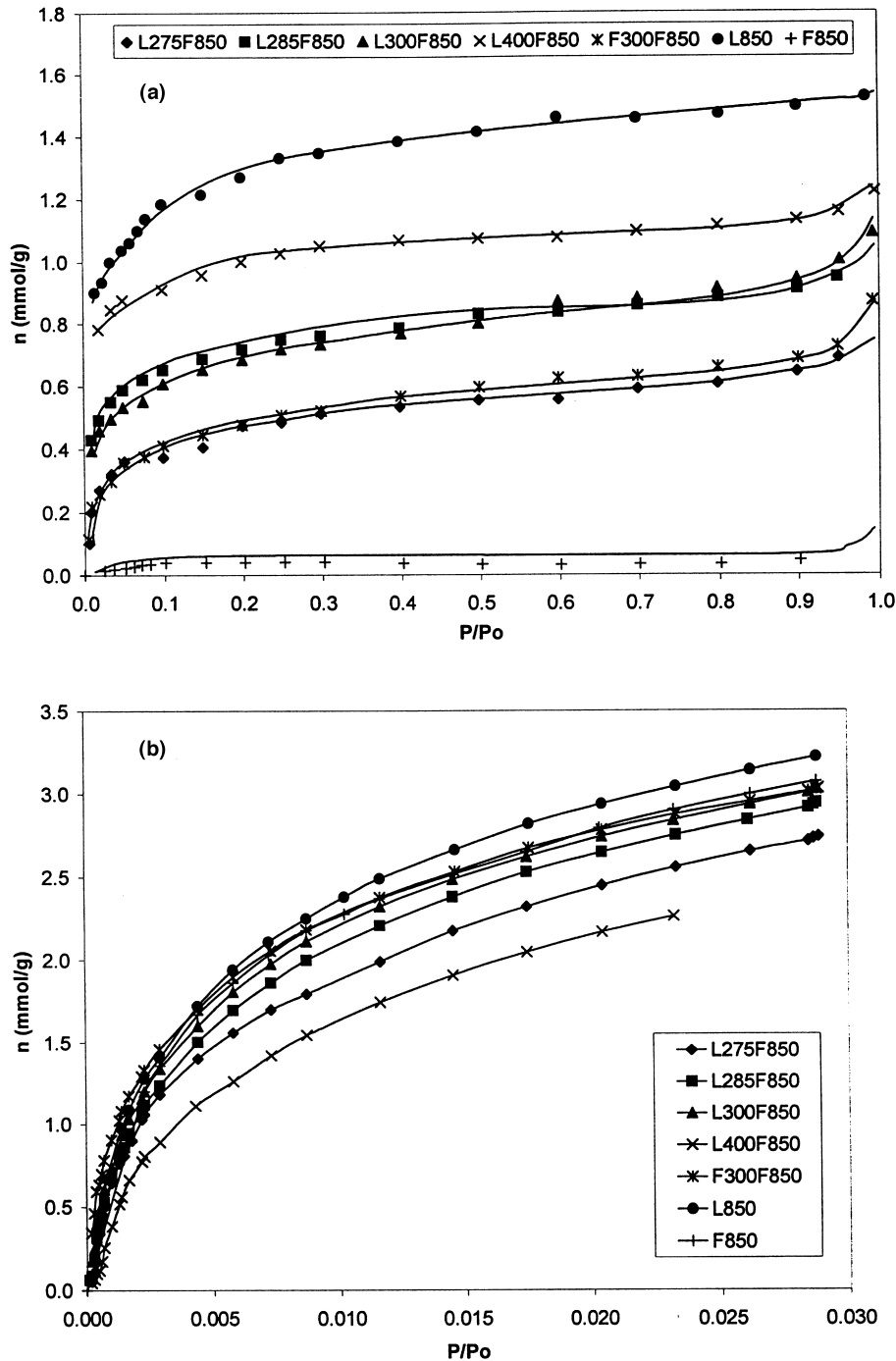


Fig. 4. Adsorption isotherms of the carbonised samples: (a) N_2 ; (b) CO_2 .

than that of sample F850A5. Therefore, an increase in the heating rate produces a decrease in the mechanical resistance of the activated carbons obtained.

In the micrographs of Fig. 8, the different textures

between the low-density sample L300F850 and the high-density sample L400F850 can be observed. The structure of the low-density samples (represented by the sample L300F850) has larger voids and larger and thinner walls

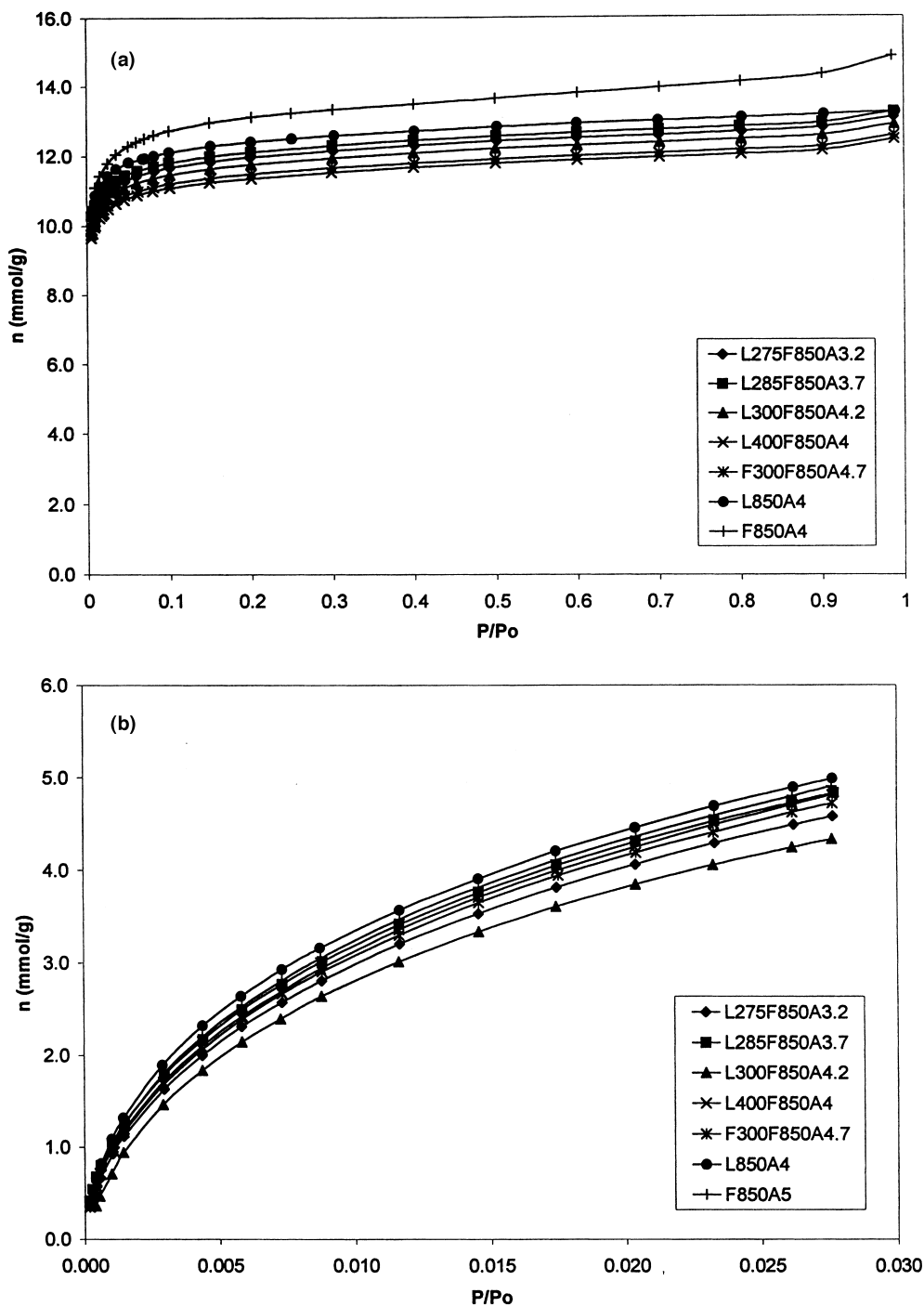


Fig. 5. Adsorption isotherms of the activated samples: (a) N_2 ; (b) CO_2 .

than sample L400F850. These observations are in good agreement with the density and mechanical strength of the samples.

In a complementary work [8], thermogravimetric analyses were carried out of the intermediate chars, and a detailed kinetic analysis was also performed. The main

Table 3

Specific surface areas of the activated and carbonised carbons (using the Dubinin-Radushkevich (D.R.) equation)

Sample	Activated carbons		Carbonised samples	
	$S_T(\text{CO}_2)$ ($\text{m}^2 \text{g}_{\text{daf}}^{-1}$)	$S_T(\text{N}_2)$ ($\text{m}^2 \text{g}_{\text{daf}}^{-1}$)	$S_T(\text{CO}_2)$ ($\text{m}^2 \text{g}_{\text{daf}}^{-1}$)	$S_T(\text{N}_2)$ ($\text{m}^2 \text{g}_{\text{daf}}^{-1}$)
L275F850A3.2	1005.9	1225.6	552.1	50.7
L285F850A3.7	1131.6	1236.0	602.7	75.2
L300F850A4.2	1005.7	1202.4	636.2	72.1
L400F850A4	1108.3	1157.4	539.9	51.6
L850A4	1175.7	1241.0	625.3	133.1
F850A5	1217.7	1315.4	514.0	4.9

conclusions of this study were that the first process in the decomposition of almond shells, corresponding to hemicellulose [9,10], is not present in any of the chars prepared. Thus, it can be concluded that all these intermediate treatments are able to decompose the main part of the hemicellulose. The second process, corresponding to cellulose decomposition [9–11], is clearly observed in the chars produced at temperatures up to 300°C, and decreases in intensity as the temperature increases. The intermediate temperatures selected are within the range of decomposition of the cellulose. If the temperature is higher, a single broad peak exists, corresponding mainly to the decomposition of the lignin.

These results support the hypothesis that a certain amount of gases (in this case mainly from the cellulose fraction) must be evolved simultaneously with weakening of the linkages of the lignin (or the remaining residue), in order to obtain low-density chars after the second treatment. On the other hand, when all the cellulose has been decomposed in the first stage, the system is not fluid enough, nor is there enough gas evolution to expand the char, and this even particle shrinking may dominate, yielding denser chars such as the L400F850.

The micrographs of Fig. 9 support this hypothesis. A large number of white spots can be observed for L285F850 at a magnification of $\times 500$. At a magnification of $\times 5000$,

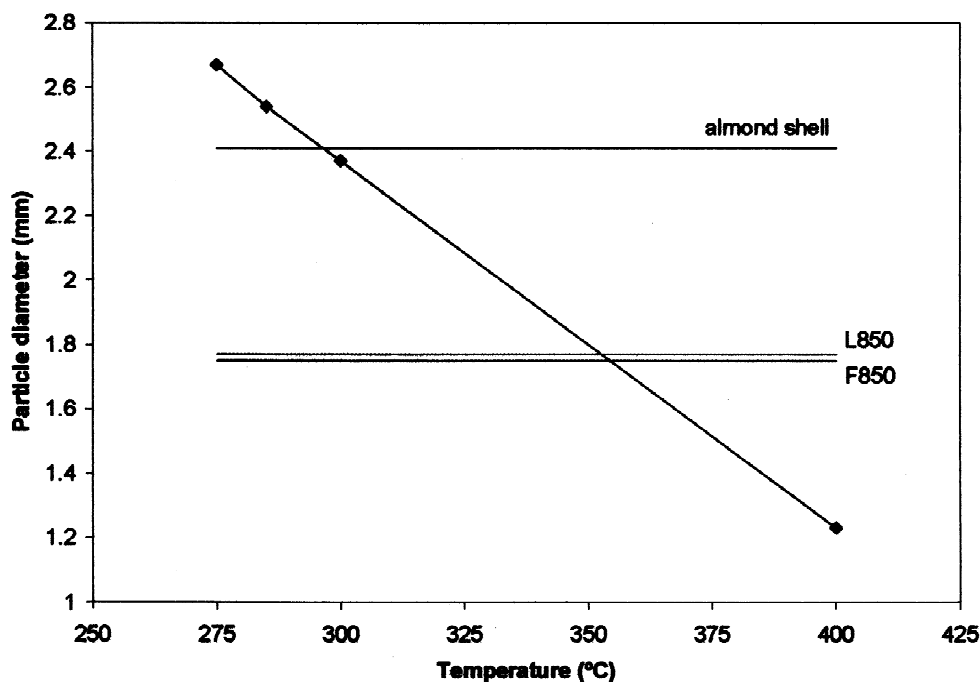


Fig. 6. Average diameter of the carbonised particles as a function of the temperature of the first stage.

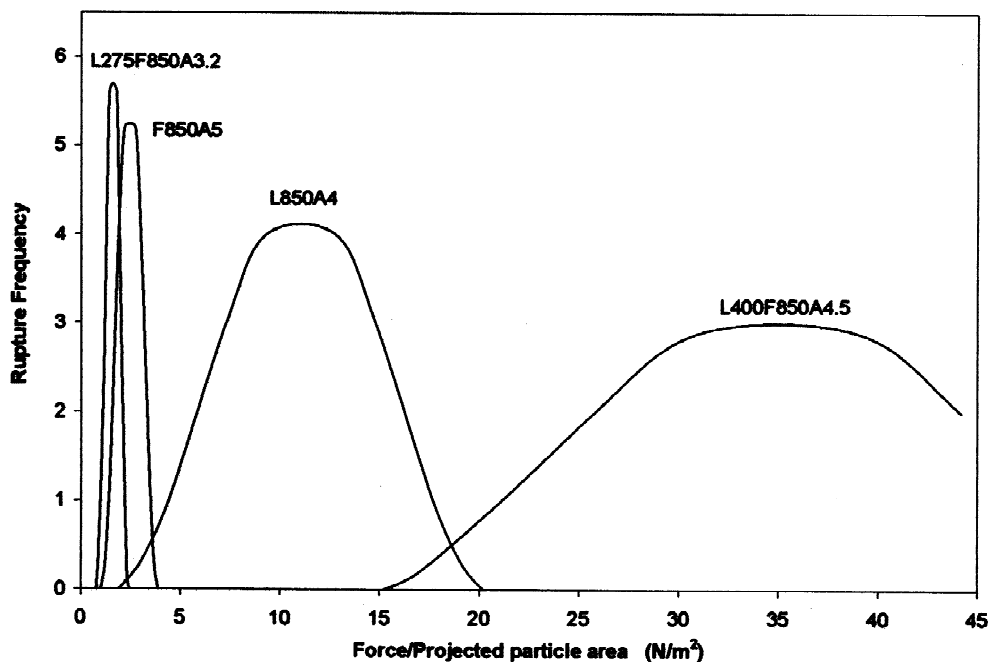


Fig. 7. Mechanical resistance of the activated samples.

such spots appear similar to craters or pores, which may act as chimneys where the evolved gases are eliminated from the char. A possible mechanism explaining these structures may involve the sample passing through a fluid phase, allowing the flow of material. Subsequent processes (most probably crosslinking processes) must also occur, where this structure is consolidated, allowing its observation. After this study it seems apparent that the very similar densities of samples L850 and F850 must be a coincidence.

3.4. Reactivity of the chars.

Fig. 10 shows the micrographs corresponding to sample F850A5 at different magnifications. Groups of white spheres can clearly be observed in these micrographs, which could be associated with coalesced ash or sintered particles. Moreover, in the micrograph shown in Fig. 11 for the same sample, the presence of 'filaments' can be observed, which may be due to previous stages of the formation of the spheres by migration, coalescence or sintering. SEM-EDX analyses of these structures (both filaments and spheres) reveal that the major component is calcium. This feature may play an important role in the reactivity of the samples. It is well known that calcium acts as an active catalyst for the CO_2 gasification of chars [12]. Both, the amount and dispersion of the catalyst are very

important in the catalysed process. SO_2 adsorption has been used to characterise the dispersion of the calcium particles [4]. Thus, in order to obtain more information about this behaviour, a study of adsorption of SO_2 for the chars L850 and F850 has been carried out. Table 4 shows the retention of SO_2 , the yield of the carbonisation process, and the percent of ash.

Although the relation of retention of SO_2 to ash is slightly higher in sample L850, it is evident that the flash treatment produces a char with a larger amount of ash of about the same degree of dispersion, and, consequently, with a larger concentration of active centres of CaO per g of char. This fact would explain the larger reactivity with the activating agent CO_2 observed in the samples obtained with a flash treatment, as compared to a low heating rate treatment.

4. Conclusions

The density of the chars from almond shells depends on the thermal treatment of the raw material. The amount of gases to be evolved during the carbonisation process, the fluidity of the residues and the processes of shrinkage and crosslinking are very important in determining the density of the chars obtained by combined or single treatments.

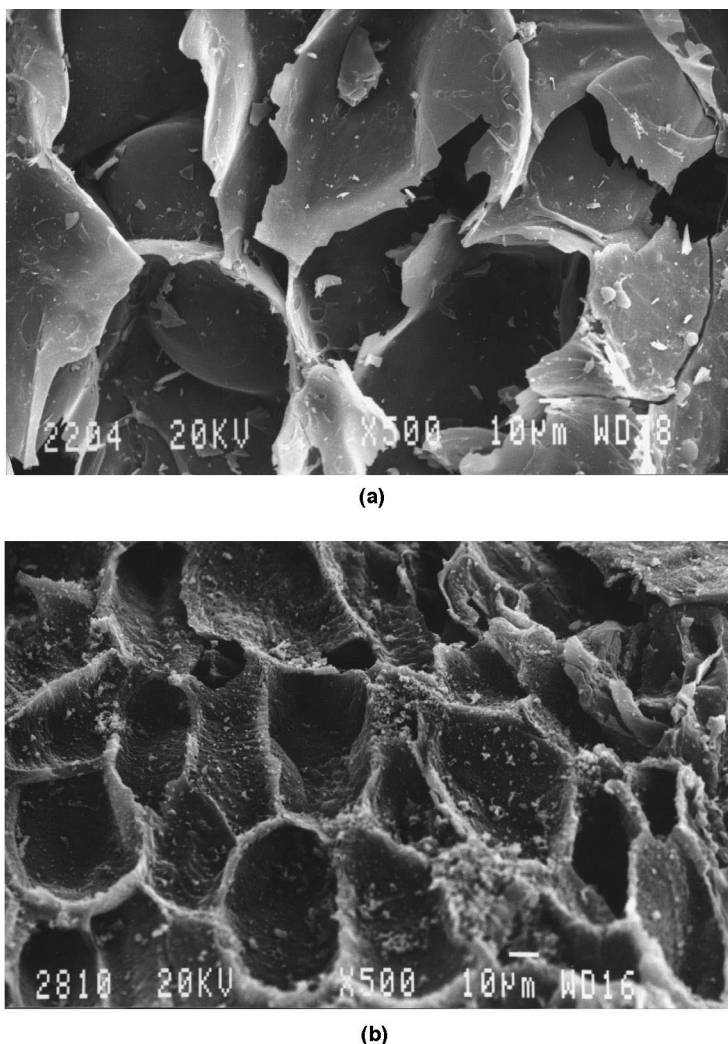


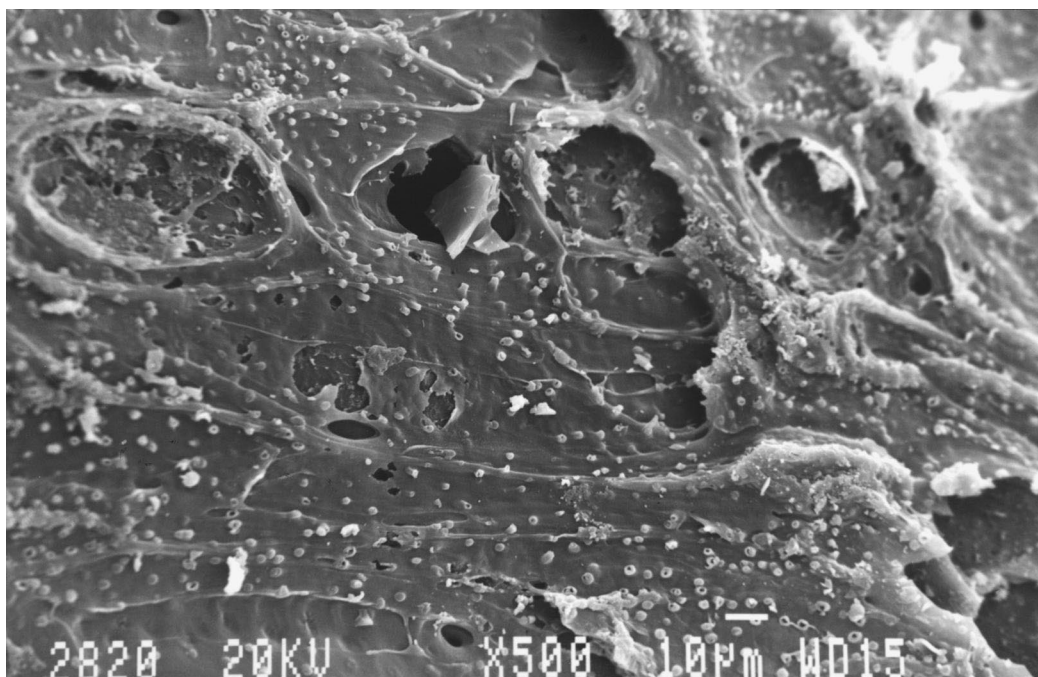
Fig. 8. SEM micrographs of the external structure of: (a) sample L300F850 at a magnification of $\times 500$; and (b) sample L400F850 at a magnification of $\times 500$.

A very interesting char (and the subsequent activated carbon) was obtained at an intermediate temperature of 400°C in the first carbonisation step, followed by a high heating rate carbonisation process up to 850°C . This char presents a higher reactivity than that obtained in a single low heating rate carbonisation process and a significantly higher density and mechanical strength. These properties are maintained in the corresponding activated carbons, which develop surface areas similar to the rest of the samples. These carbonisation conditions represent a very promising alternative to producing activated carbons from lignocellulosic materials since many of the advantages of the different thermal treatments combine.

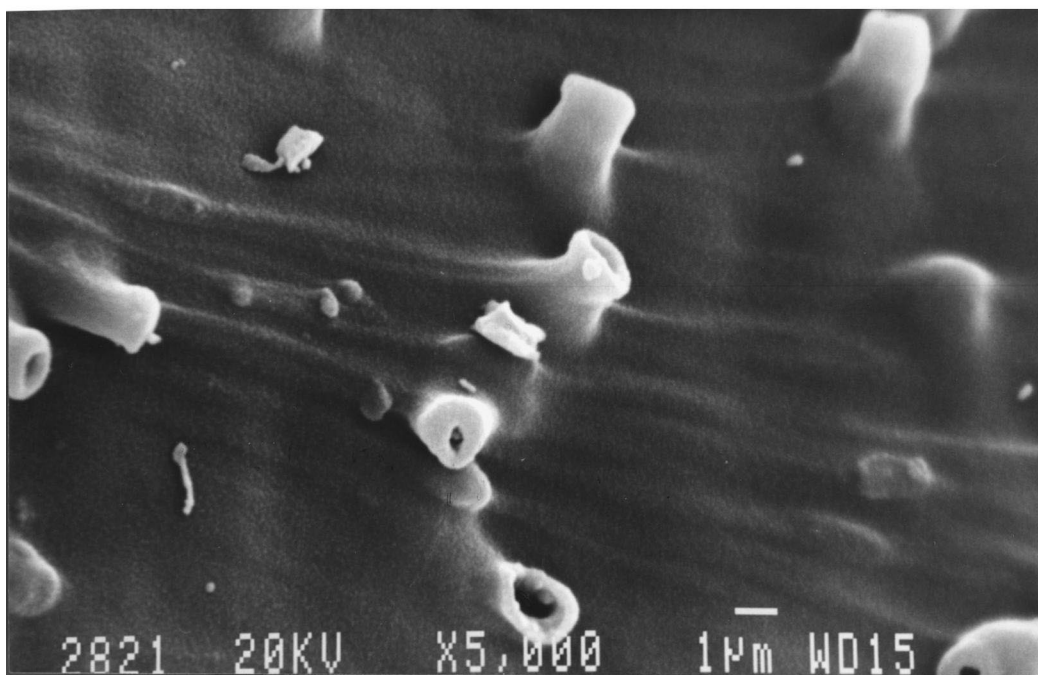
Finally, it has been observed that the surface area of the chars are not directly related to their reactivity which greatly depends, among other factors, on the amount and dispersion of the inorganic compounds present in the sample.

Acknowledgements

Support for this work was provided by the Ministerio de Educación y Cultura, Dirección General de Enseñanza Superior, research project no. PB96-0329.

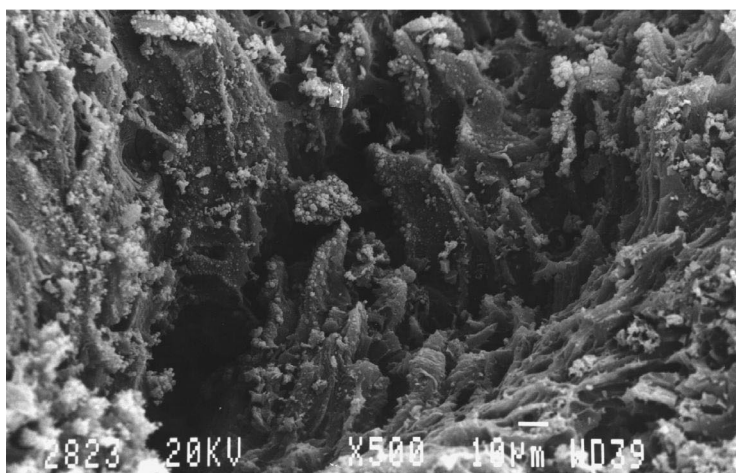


(a)

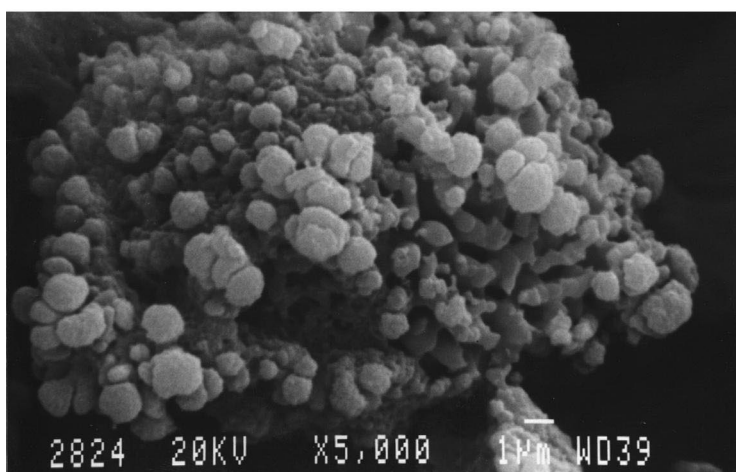


(b)

Fig. 9. SEM micrographs of the external structure of sample L285F850 at magnifications: (a) $\times 500$; and (b) $\times 5000$.



(a)



(b)

Fig. 10. SEM micrographs of the external structure of sample F850A5 at magnifications: (a) $\times 500$; and (b) $\times 5000$.

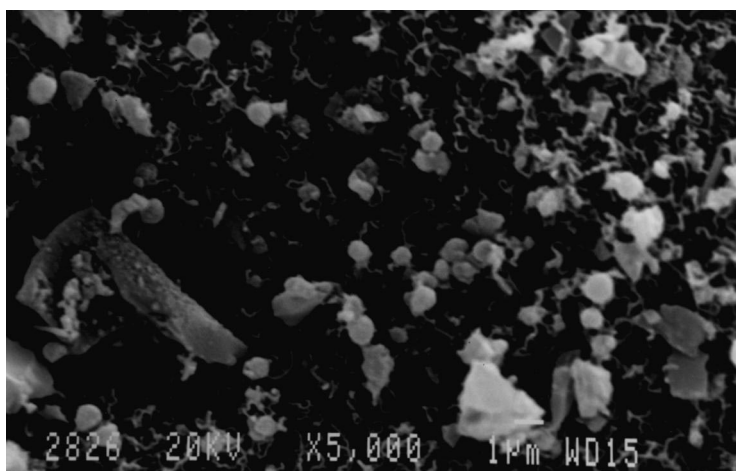


Fig. 11. SEM micrographs of the external structure of sample F850A5 at a magnification of $\times 5000$.

Table 4

Retention of SO₂, yields of carbonisation and percent ash of chars L850 and F850

Sample	Y _G (%)	Ash (%)	mg SO ₂ /g _{carbon}	mg SO ₂ /ash
L850	27.04	1.6	11.1	6.94
F850	16.22	2.7	17.0	6.33

References

- [1] Rodriguez Reinoso F, Linares Solano A. In: Thrower PA, editor, Chemistry and physics of carbon, Vol. 21, New York: Dekker, 1988, pp. 1–146.
- [2] Marcilla A, Asensio M, Martín-Gullón I. Carbon 1996;34(4):449–56.
- [3] Garcia AN, Font R, Marcilla A. Energy and Fuels 1995;9:648–58.
- [4] Macías Pérez MC, Eliminación de SO₂ en efluentes gaseosos mediante CaO soportado en carbones activos, PhD thesis, University of Alicante, 1997.
- [5] Mackday DM, Roberts PV. Carbon 1982;20(2):95–104.
- [6] Gonzalez MT, Rodriguez-Reinoso F, Garcia AN, Marcilla A. Carbon 1997;35(1):159–65.
- [7] Dubinin MM, Stoeckli HF. J Colloid Interface Sci 1980;75(1):34–43.
- [8] Marcilla A, Asensio M, García-García SM, Conesa JA, Thermal treatment and foaming of chars obtained from almond shells. Kinetic study, Fuel, in press.
- [9] Caballero JA, Conesa JA, Marcilla A. J Anal Appl Pyrol 1997;44:75–88.
- [10] Conesa JA, Marcilla A, Caballero JA. J Anal Appl Pyrol 1997;43:59–69.
- [11] Caballero JA, Conesa JA, Font R, Marcilla A. J Anal Appl Pyrol 1997;42:159–75.
- [12] Wood BJ, Sancier KM. Catal Rev Sci Eng 1984;26:233–79.